



Contents lists available at ScienceDirect

Science of the Total Environment

journal homepage: www.elsevier.com/locate/scitotenv

Alternaria spore exposure in Bavaria, Germany, measured using artificial intelligence algorithms in a network of BAA500 automatic pollen monitors



Mónica González-Alonso ^{a,b,1}, Mihai Boldeanu ^{c,1}, Tom Koritnik ^d, Jose Gonçalves ^{d,e,f}, Lenz Belzner ^g, Tom Stemmler ^h, Robert Gebauer ^{a,i}, Łukasz Grewling ^j, Fiona Tummon ^k, Jose M. Maya-Manzano ^a, Arturo H. Ariño ^b, Carsten Schmidt-Weber ^a, Jeroen Buters ^{a,*}

^a Center of Allergy & Environment (ZAUM), Technical University/Helmholtzzentrum Munich, Member of the German Center for Lung Research (DZL), Munich 80802, Germany

^b University of Navarra, Environmental Biology and BIOMA, Pamplona 31008, Spain

^c Polytechnic University of Bucharest, CAMPUS lab, Bucharest 060042, Romania

^d National Laboratory of Health, Environment and Food, Ljubljana 1000, Slovenia

^e Institute of Sustainable Processes of the University of Valladolid, Valladolid 47011, Spain

^f University of Valladolid, Department of Chemical Engineering and Environmental Technology, Valladolid 47011, Spain

^g Technische Hochschule Ingolstadt, Esplanade 10, Ingolstadt 85049, Germany

^h Helmut Hund GmbH, Wetzlar 35580, Germany

ⁱ IT consulting Robert Gebauer, Germany

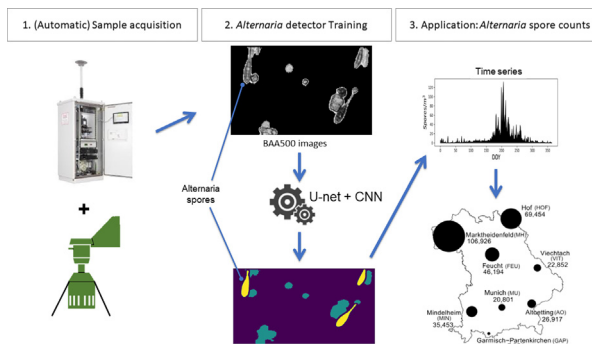
^j Adam Mickiewicz University, Laboratory of Aerobiology, Department of Systematic and Environmental Botany, Poznań 61-712, Poland

^k Federal Office of Meteorology and Climatology (MeteoSwiss), Payerne CH-1530, Switzerland

HIGHLIGHTS

- About 6 % of the European population is sensitized to airborne *Alternaria* spores.
- Need of reliable spore's (here automatic) monitoring in a climate change scenario
- Development and validation of an algorithm to detect *Alternaria* spores.
- Automatic re-analysis of the historical database to obtain a complete time series.
- Detection of a latitudinal gradient of *Alternaria* spores in Bavaria, South-Germany

GRAPHICAL ABSTRACT



ARTICLE INFO

Editor: Anastasia Paschalidou

Keywords:

Alternaria
Fungal spores
Allergy
Automatic monitors
Convolutional neural networks
U-net

ABSTRACT

Although *Alternaria* spores are well-known allergenic fungal spores, automatic bioaerosol recognition systems have not been trained to recognize these particles until now. Here we report the development of a new algorithm able to classify *Alternaria* spores with BAA500 automatic bioaerosol monitors. The best validation score was obtained when the model was trained on both data from the original dataset and artificially generated images, with a validation unweighted mean Intersection over Union (IoU), also called Jaccard Index, of 0.95. Data augmentation techniques were applied to the training set. While some particles were not recognized (false negatives), false positives were few. The results correlated well with manual counts (mean of four Hirst-type traps), with $R^2 = 0.78$. Counts from BAA500 were 1.92 times lower than with Hirst-type traps.

Abbreviations: CNN, convolutional Neural Network; ASIn, Annual Spore Integral.

* Corresponding author at: Biedersteinerstrasse 29, 80802 Munich, Germany.

E-mail address: buters@tum.de (J. Buters).

¹ These authors contributed equally to this work

<http://dx.doi.org/10.1016/j.scitotenv.2022.160180>

Received 8 September 2022; Received in revised form 9 November 2022; Accepted 10 November 2022

Available online xxx

0048-9697/© 2022 Elsevier B.V. All rights reserved.

Classification
Time series

The algorithm was then used to re-analyze the historical automatic pollen monitoring network (ePIN) dataset (2018–2022), which lacked *Alternaria* spore counts. Re-analysis of past data showed that *Alternaria* spore exposure in Bavaria was very variable, with the highest counts in the North (Marktheidenfeld, 154 m a.s.l.), and the lowest values close to the mountains in the South (Garmisch-Partenkirchen, 735 m a.s.l.). This approach shows that in our network future algorithms can be run on past datasets. Over time, the use of different algorithms could lead to misinterpretations as stemming from climate change or other phenological causes. Our approach enables consistent, homogeneous treatment of long-term series, thus preventing variability in particle counts owing to changes in the algorithms.

1. Introduction

Allergy has become an important health issue over the last decades and currently about 20 % of the worldwide population suffers from some kind of allergy (Pawankar, 2014). Because the prevalence of pollinosis in Europe has been reported to be around 40 % (D'Amato et al., 2007), many studies have focused on pollen allergies, but allergic reactions can also be caused by fungal spores.

Fungal allergies are still a largely unexplored field, in part due to the lack of airborne spore monitoring (Bozek and Pyrkosz, 2017; Cramer et al., 2014; Kasprzyk et al., 2015; Martinez-Canavate Burgos et al., 2007; Tabar et al., 2008) stemming from the more difficult manual spore counting as compared to pollen. In addition, the dominance of *Cladosporium* spores' results in laborious, tedious and unpopular (i.e. not suitable for particles to count).

Alternaria spp. is a ubiquitous saprophytic fungus, one of the four main fungal allergenic genera, along with *Aspergillus*, *Aspergillus* and *Penicillium* (D'Amato et al., 1997; Bozek and Pyrkosz, 2017). Sensitization to molds may already start in childhood and its symptoms are the same as for pollinosis: allergic rhinitis and/or asthma (D'Amato et al., 1997; Delfino et al., 1996; Forkel et al., 2021; Grinn-Gofroń et al., 2011; Kasprzyk et al., 2015; Simon-Nobbe et al., 2008; Spieksma, 2003; Twaroch et al., 2015). The threshold for the start of symptoms by *Alternaria* spores is calculated to be about 100 spores/m³ (Twaroch et al., 2015).

Allergy to *Alternaria* coincides with the period when their conidia are present in the air, which mainly happens during the summer and the early autumn. Spore levels are positively correlated with higher temperature, lower humidity and windy days (two days before their release), and negatively correlated with precipitation (Grinn-Gofroń et al., 2011). This is why *Alternaria* spores are called 'dry' spores (Spieksma, 2003). In Europe, prevalence of *Alternaria* allergies varies along a latitudinal gradient, with a lower incidence in northern countries (2–3 %) and higher prevalence in Mediterranean countries, with the highest incidence in Spain and Greece (around 20 %) (D'Amato et al., 1997; Damialis et al., 2015a; Damialis et al., 2015b). In Spain, *Alternaria* spores show a bimodal behavior with two peaks during the season (Maya-Manzano et al., 2012; Picornell et al., 2022).

Because fungal spore concentrations in the air partly coincide with the pollen season, it is sometimes difficult for allergologists to make the correct diagnosis of a fungal spore allergy. This is further complicated by the fact that allergy to molds frequently appears in multi-sensitized patients (Lizaso Bacaicoa et al., 2003; Twaroch et al., 2015; Vidal et al., 2014). With an accurate diagnosis it is possible to personalize medication or immunotherapy, avoiding wrong immunotherapy will improve the patients' quality of life and reduce other side effects of allergic diseases, such as economic impacts due to absence from work (Kasprzyk et al., 2019).

The hallmark of allergy diagnosis is a provocation test by the eliciting compound. This is however time consuming and costly, and is not popular in general medical practice. Knowing airborne spore concentrations and correlating this with patients' symptoms, either online or with a hand-written diary, improves diagnosis (Lizaso Bacaicoa et al., 2003; Tabar et al., 2008; Twaroch et al., 2015). Thus, monitoring of airborne concentrations is a valuable tool that can help allergists, for example by enabling the linking of spore exposure data with patients' symptoms, thus reducing the need for provocation tests.

Until now, Hirst volumetric pollen traps have been the main pollen monitoring devices throughout Europe (Buters et al., 2018; Hirst, 1952). However, the methodology is highly time-consuming and requires expert's knowledge to identify particles. In addition, results appear with a delay from 7 to 10 days (Tummon et al., 2021a, 2021b).

In the last fifteen years, automatic pollen monitoring devices have appeared on the market, with most becoming available only in the past 5 years. These devices are capable of classifying pollen based on different technologies (i.e. image or holographic recognition or fluorescence) and provide real-time or near real-time airborne concentrations (Chappuis et al., 2020; Oteros et al., 2020; Šaulienė et al., 2019; Šaulienė et al., 2021; Sauvageat et al., 2019; Tešedić et al., 2020). Currently they are not yet used operationally to classify fungal spores, although some success has been achieved for short test periods (Erb et al., 2022).

Since 2018, Bavaria (Germany) has the first fully automatic pollen monitoring network worldwide (www.ePIN.bayern.de, accessed April 2022) composed of eight BAA500 (Helmut Hund GmbH, Wetzlar, Germany) automatic pollen monitors, able to count >30 different taxa (Oteros et al., 2015, 2020). The device is an image recognition-based system that collects ambient air at a rate of 1120 L/min. Airborne particles impact on a sticky plate and stacks of images with different optical depths are taken with a camera attached to a microscope. These stacks are then condensed to one synthetic (2D) image that is stored in an online database. Software then determines what part of the image is a pollen grain, an inorganic particle or a spore, and then also stores the particle's identity (Fig. 1).

Deep learning (DL) techniques have rapidly evolved over the last decades and are able to accomplish many tasks, including detecting objects in images (Schmidhuber, 2015). Convolutional Neural Networks (CNNs) were the best performers in the ImageNet classification challenge (Krizhevsky & Sutskever, 2012) and later, when applied to object detection tasks (Girshick et al., 2014; Szegedy et al., 2013). Therefore, they have been employed in multiple fields, including pollen classification (Khanzhina et al., 2022; Polling et al., 2021; Sevillano et al., 2020; Sauvageat et al., 2019). One of such CNNs is the U-net, initially developed to detect cells (Ronneberger et al., 2015), but that has been widely used in many applications in various fields, as in Abascal et al. (2022).

Although *Alternaria* spores are easily recognized in the synthetic images of the BAA500 by eye, the existing algorithms were not trained to correctly classify and report their concentrations.

Here we developed an algorithm based on the U-net architecture to widen the classifying capability of the BAA500 by additionally detecting *Alternaria* spores. Moreover, this tool also worked to re-analyze the image database to generate a complete and homogeneous time series, i.e. for all devices in Bavaria since their installation. Our work also validated the algorithm against the results of manual analysis from Hirst-type pollen monitors, currently considered as the only reference in Aerobiology.

2. Materials and methods

We processed real-life images produced by BAA500 monitors. Every 3 h, a microscope-camera photographs about 144 regions of the sticky plate, each region being a single stack of approximately 210 images per region in the z-axis. Then, software condenses the images into one synthetic (2D), grayscale 1280 × 960-pixel image per stack ("raw images"), removing the background. Particles are detected and classified as either pollen,

D'Amato

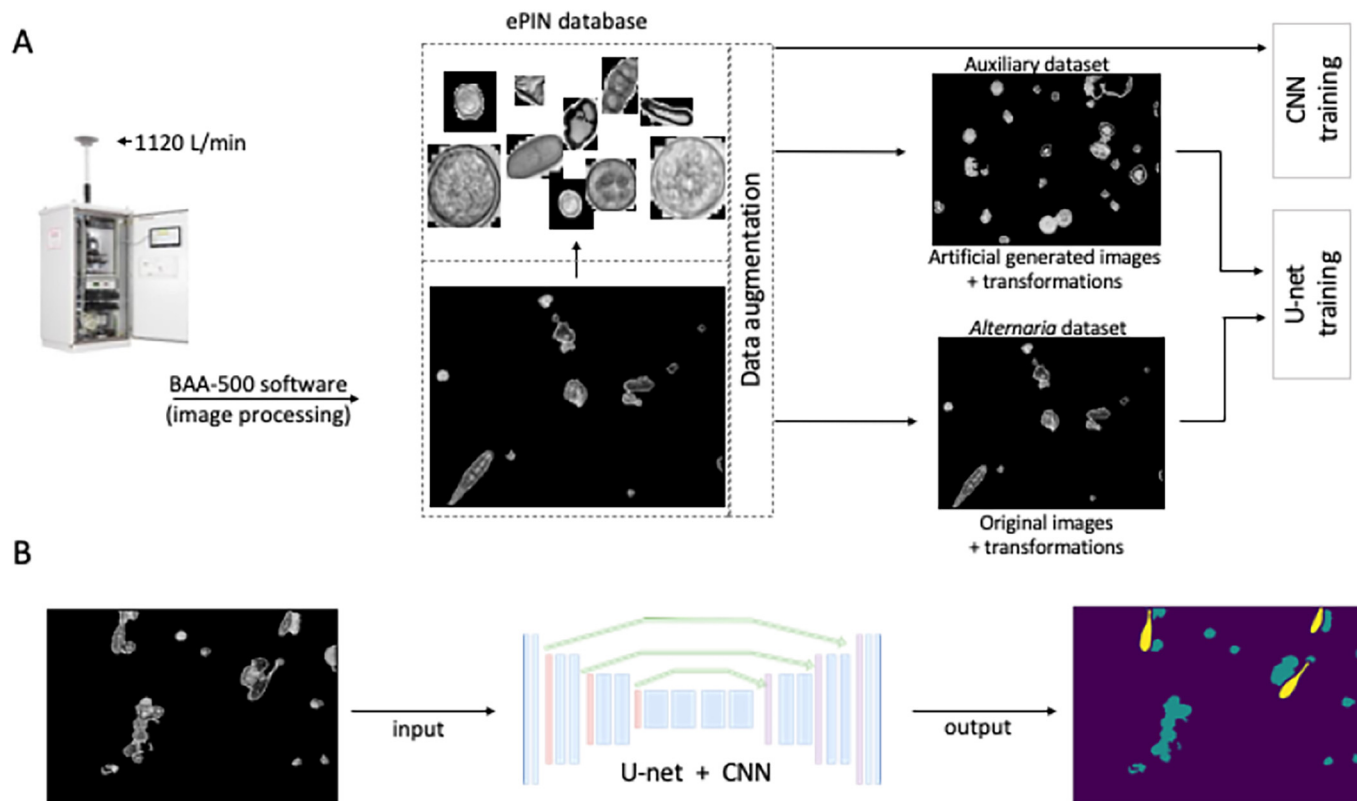


Fig. 1. Automatic image recognition workflow. The BAA500 sucks in 1120 L/min and particles impact onto a round sticky plate. Every 3 h, a microscope-camera photographs around 144 regions of the plate, taking a stack of approximately 210 images per region in the z-axis. Software then condenses the images into one synthetic (2D) image per stack, removing the background. Synthetic images and coordinates of all the particles detected are stored in the ePIN database. Data augmentation techniques were applied to both datasets and used to train the U-net. A second CNN confirmed the output of the U-net. (B) Synthetic images (2D) produced by BAA500 are analyzed by the U-net algorithm and the CNN. Output shows (in this case) *Alternaria* spores as yellow patches.

fungal spores, or as non-pollen particles. All images and the detected particles' coordinates are stored in a No-SQL database (Fig. 1).

2.1. *Alternaria* dataset and Auxiliary dataset

Our focus in this work was on identifying *Alternaria* spores, which are currently not identified in the ePIN network and are usually classified as “non-pollen particles”. We started by compiling an *Alternaria* spore image collection (“*Alternaria* dataset”) from a sub-sample of 2689 images that contained *Alternaria* spores, mainly from the months of July and August, when *Alternaria* spores are airborne at high levels.

Then, images were annotated with the VGG Image Annotation (VIA) 2.0.10 open software (Dutta et al., 2019). To reduce additional error sources on the training set, fourteen people worked on the annotation task creating segmentation masks by surrounding each spore with the annotation tool. All annotations were manually checked by experts before their use for the training, and resulted in a set of >3000 annotations of *Alternaria* spores. The dataset contained masks for two more automatically-labeled classes as well: other particles (not *Alternaria*) and background.

An additional dataset of particles captured and classified with the BAA500 software (“Auxiliary dataset”) was created by selecting particles from the ePIN database which were manually checked by experts during a previous validation process. Furthermore, these images were re-validated by other experts before their use to exclude any misclassifications made by the manual counters. This Auxiliary dataset (with double expert classification) contained samples of cropped particles, whose sizes depended on the particle content. Therefore, images were resized to 360×360 pixels before use to train a second Convolutional Neural Network (CNN) (see section 2.4), and also to enlarge the 3000-image hand-crafted dataset by artificially generating images similar to the raw images.

2.2. Metrics

To evaluate the performance of the model for the detection of *Alternaria*, multiple metrics were selected.

Because the selected network operates at pixel level, during training we used the pixel accuracy and the unweighted mean Intersection over Union (IoU), also called Jaccard Index (Minae et al., 2020).

While the pixel accuracy metric informs us about the percentage of pixels that are correctly classified in each image, the information is distorted by the fact that most pixels represent empty space or particles other than *Alternaria*, overestimating the actual performance of the model. The IoU, on the other hand, looks only at the True Positives and ignores the True negatives (mostly background pixels), which would inflate the performance when looking just at the *Alternaria* class. As a measure of performance when using the model to get the number of events of *Alternaria* spores detected per image we used the recall, precision and F1 score metrics.

Results were True positive (TP) if an image contained an *Alternaria* spore and the model detected it. If instead another non-*Alternaria* particle was classified as an *Alternaria* spore this was considered a false positive (FP). If the algorithm missed an *Alternaria* spore this was considered a false negative (FN). The true negatives were not computed because most images and particles are True negatives (background and junk). The goodness-of-fit metrics were calculated as:

$$IoU \text{ score} = \frac{TP}{(TP + FP + FN)}$$

$$Precision = \frac{TP}{(TP + FP)}$$

$$\text{Recall} = \frac{TP}{(TP + FN)}$$

$$F1 \text{ score} = \frac{2 * \text{precision} * \text{recall}}{(\text{precision} + \text{recall})}$$

Because the classes present in the datasets are highly imbalanced, with the *Alternaria* class having the least number of pixels over the dataset ($37 * 10^5$, 1 %) compared to other particles ($70 * 10^5$, 2 %) and background ($5 * 10^6$, 97 %), the use of weights is required when training to prioritize the *Alternaria* class over the others.

2.3. Data augmentation

When using deep CNNs, the size of the training set is one of the most important parameters that will influence the performance of the model. To alleviate the problem of not having enough samples, data augmentation approaches can be used to create “new” images from the ones we already had and therefore, to avoid overfitting (Boldeanu et al., 2022; Krizhevsky & Sutskever, 2012; Shorten and Khoshgoftaar, 2019).

In our work, the generation of new training samples was split into two main types: i) augmenting the hand-picked images by applying randomly the classical transformations of changing the position, the brightness or applying a deformation to the images (Fig. 2-A) and ii) creating artificial synthetic samples by compositing images from elements of the Auxiliary dataset to generate images similar in size and complexity to real ones (Fig. 2-B). Classical techniques were also applied randomly to these artificially generated images during the training step.

2.4. Selected architecture and post-processing results

The U-net network architecture is widely used for the task of segmentation in the medical and biological fields (Ronneberger et al., 2015), due to its ability to learn complex patterns that enable users to do class segmentation on complex images or image-related datasets.

Several strategies were employed to find the best training approach, alternating images with and without data augmentation techniques: i) training with only raw images to get a baseline, ii) training with augmentation on the raw images, iii) training with augmentation on the artificially-generated samples, iv) doing a mixed training of real images with augmentations + artificially-generated images with augmentations. For every combination, the training dataset was split into training (80 %), validation (10 %) and test (10 %) sets.

During training, regularization was used to constrain the magnitude of the weights (Bishop, 1996). Because the data was highly imbalanced (many more non-*Alternaria* than *Alternaria* particles, as mentioned above), sample weight masks were used to make the model focus on the *Alternaria* patches in the image. The model was evaluated after each epoch of training with the validation set.

Since the U-net is a fully convolutional network, where the output is a segmentation mask with pixel-level classification (Fig. 3), some post-processing is required.

The post-processing method consisted of cropping around the detected *Alternaria* masks and passing them through a second convolution-based model, a modification of the VGG-19 architecture (Simonyan and Zisserman, 2015), to confirm that the mask was actually an *Alternaria*, thus reducing eventual FPs. This second CNN was trained with images from the Auxiliary dataset, thus containing one particle, and able to discriminate up to 19 classes (18 pollen types + *Alternaria* spores). Finally, we used a connected components method to count the number of patches of *Alternaria* spores within every image.

For additional technical details, see Boldeanu et al. (2022). The code of both the U-net and the CNN can be made available on request.

2.5. U-net + CNN testing and implementation

The feasibility and outcome of the U-net + CNN were evaluated along four step-wise operations in the workflow. In the first step we optimized the performance of the algorithm on the training dataset.

In the second step we validated the model using data from different locations of the ePIN network, also to detect any possible data drift between the different BAA500 devices and to ensure that the model generalized well without overfitting over the training dataset. Two tests were conducted (Test 1 and Test 2), taking as input two sub-samples of images with no annotations from the ePIN database.

First, we tested the network with 1000 random images from each of the eight stations of the ePIN network. All images were from the 10th of July, from any year in the 2018–2020 range (Test 1). The date was randomly selected among summer days with confirmed presence of *Alternaria* in the atmosphere, allowing evaluation of the model. Secondly, we took 2000 random images from the eight ePIN locations in Bavaria from different days and years, to confirm there was no bias due to the choice of the training set (compiled mainly of images from the months of July and August) (Test 2). The output of all test images was manually checked by experts.

A third additional step (Test 3) was to evaluate the ability of the model to count spores, compared to the classical manual method (mean of four Hirst traps, the standard instrument for pollen monitoring). Validation

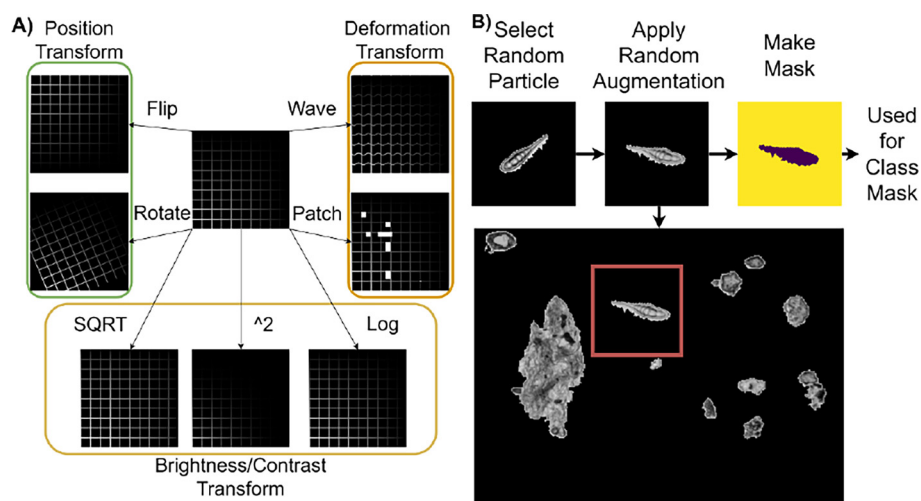


Fig. 2. Types of data augmentation applied to the training set. A) Classical image transformations: position transform, deformation transform and brightness/contrast transform augmentations. B) Synthetic image generation with BAA500 detected particles (pollen grains, inorganic particles, fungal spores).

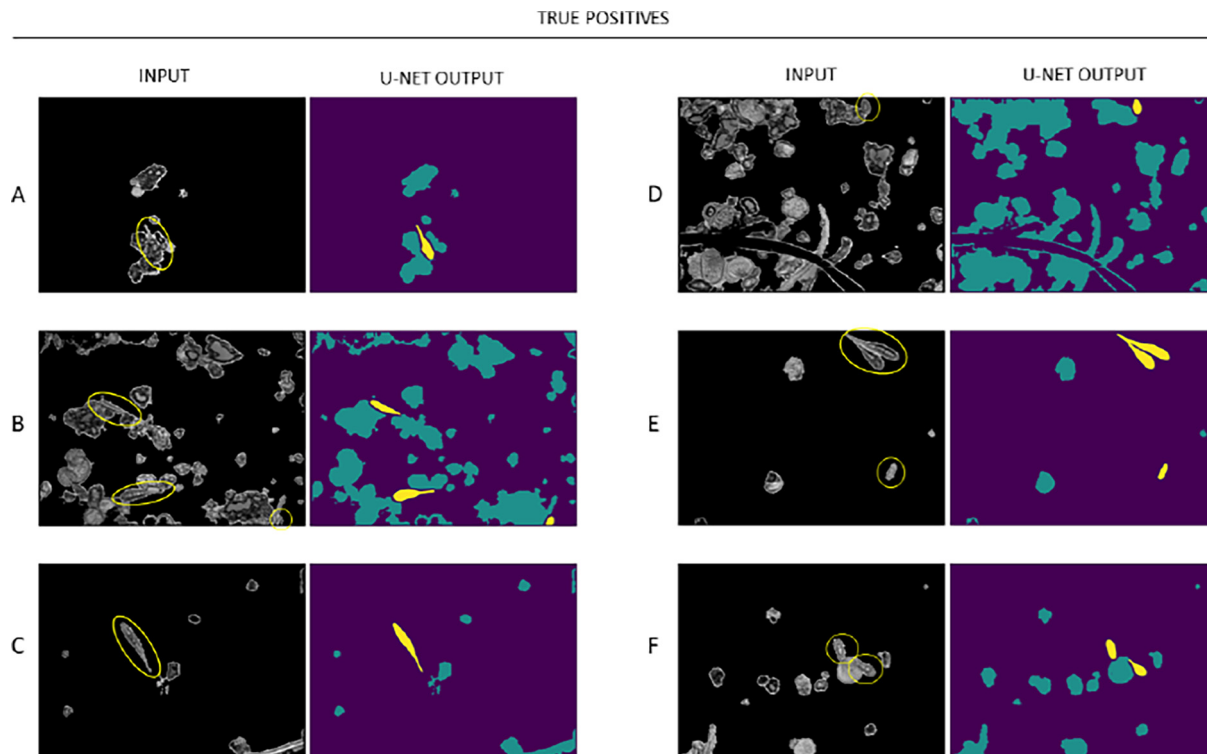


Fig. 3. Output examples of the U-net for *Alternaria* spores. A-F Left: black and white synthetic images, produced by the BAA500 software that are used as input for the U-net. In these, ground truth *Alternaria* spores are marked with a yellow circle. A-F Right: output of the U-net, *Alternaria* spores detected marked as yellow patches.

was carried out using data from the ‘EUMETNET AutoPollen-COST ADOPT intercomparison campaign 2021 (AIC)’, which took place in Munich as part of the EUMETNET Autopollen project (Clot et al., 2020). This campaign was held during the spring season of 2021 to evaluate all available automatic monitors and compare them to data from manual Hirst pollen traps. Although their accuracy is debated, particularly at low atmospheric concentrations, Hirst-type traps are still considered the reference device in airborne pollen and spore monitoring (Oteros et al., 2017; Tummon et al., 2021b). The campaign ran from 3.03.2021 to 15.07.2021 and the BAA500 was run in parallel to four Hirst-type pollen traps whose mean was taken as a reference to validate the results of our algorithm.

The last step was to actually use the model on a large dataset (from the eight ePIN stations, over the years 2018–2021) to obtain *Alternaria* time series since 2018, data that was previously analyzed by an algorithm not able to recognize *Alternaria*.

3. Results

3.1. Training results on dataset

To obtain the best training strategy and best performing model, different experiments were done with and without data augmentation. The combination of raw images with artificial-generated images, applying classical data augmentation techniques, gave the best model performance scores, with a precision of 0.91, a recall of 0.94, a F1 score of 0.93 and a validation mean IoU value of 0.95 (Table 1).

The accuracy metric for all the training strategies was at 0.99. These results are an example of why accuracy alone is not a good metric when doing segmentation of imbalanced classes.

3.2. Results from Test 1 and Test 2

The results of all images from Test 1 were manually checked and yielded a precision = 0.9, recall = 0.88 and F1 score = 0.89 (Table 1). After Test 2,

Table 1
Metrics' results on Training and Tests of the *Alternaria* detector algorithm.

		U-net training (6189 images; Jul-Aug; all ePIN stations)						
		ALT	TP	FP	FN	Precision	Recall	F1 score
TOTAL		478	452	41	26	0.92	0.95	0.93
%		100	94.6	8.6	5.4			
		Test 1 (8000 images; 10th July; all ePIN stations)						
		ALT	TP	FP	FN	Precision	Recall	F1 score
TOTAL		219	193	22	26	0.9	0.88	0.89
%		100	88.1	10	11.9			
		Test 2 (2000 images; random dates; all ePIN stations)						
		ALT	TP	FP	FN	Precision	Recall	F1 score
TOTAL		133	107	12	26	0.92	0.84	0.88
%		100	80.5	9	19.6			
		Test 3 (5725 images; 01.06.21–14.07.21; AIC ^a Munich)						
		ALT	TP	FP	FN	Precision	Recall	F1 score
TOTAL		716	656	61	60	0.92	0.92	0.92
%		100	91.6	8.5	8.4			

Table 1. Output evaluation parameters of the U-net algorithm. Different stages of training (with known images) and tests and validation (with unknown images) are shown. All images used for evaluation were 100 % hand-scored for *Alternaria* spp. and belonged to the automatic pollen monitoring network of Bavaria, Germany (ePIN database). ALT: Total *Alternaria* spores present in the images; TP (true positives): *Alternaria* spores detected by the U-net; FP (false positives): Other particles classified as *Alternaria*; FN (false negatives): manual labeled *Alternaria* spores not detected by the U-net. Precision: TP/(TP + FP); Recall: TP/(TP + FN); F1 score: $2 * (\text{precision} * \text{recall}) / (\text{precision} + \text{recall})$.

^a AIC: EUMETNET AutoPollen-COST ADOPT intercomparison campaign, Munich (Germany) (Maya-Manzano & et al., 2022).

400 (20 %) of the output images were manually checked. The results of Test 2 were a precision = 0.92, recall = 0.84, and F1 score = 0.88 (Table 1).

3.3. Results of Test 3, data validation during the 'EUMETNET AutoPollen-COST ADOPT Intercomparison Campaign (AIC)' – 2021

In the third validation step we evaluated both the performance of the algorithm and its correlation with the manual Hirst counts. First, we studied the U-nets performance when detecting *Alternaria* spores. A total of 5725 images (7 %) of the AIC were manually evaluated by experts. The selected images included all images with *Alternaria* events (725) plus 1000 '*Alternaria*-empty images' chosen randomly from each month of the campaign (February to June). We obtained a score of 0.92 in all parameters evaluated: precision, recall and F1 score (Table 1).

Afterwards we compared the BAA500 *Alternaria* counts versus the Hirst data. Two experienced technicians had manually counted *Alternaria* spores as hourly values in the Hirst trap's samples for the period 01.06.2021–14.07.2021. Spore concentrations were calculated considering the area of the slide sampled, the microscopic field and by applying a correction factor for the flow according to flow measurements during the AIC, to assure a 10 L/m² flow rate as is recommended by the standards (Galán et al., 2014; Triviño et al., 2022; Maya-Manzano et al., 2022). The manual counts from the Hirst trap data (Fig. 4-A) were aggregated into three-hour periods to compare the series with the *Alternaria* data from the BAA500 (Fig. 4-B).

The algorithm detects events from the images not concentrations. To obtain the concentration of spores in the air (spores/m³) we multiplied the raw counts (events) by a 5.5 concentration factor, calculated from the flow, impact surface of particles and percentage of the surface sampled by the BAA500 camera, (i.e. flow calculation, not a scaling factor). The resulting correlation between BAA500 and the mean of the four Hirst traps was $R^2 = 0.78$ (Fig. A.1).

3.4. Results from the historical ePIN dataset

After the validation of the algorithm against the Hirst traps during the AIC, we re-analyzed the historical ePIN database for *Alternaria* levels in Bavaria since the installation of the automatic devices (2018–2022). Here we present the distribution of *Alternaria* spores over Bavaria for the year

2021 in the ePIN network as this was a complete year with data from all eight stations.

Fig. 5-A shows the annual sum of daily mean concentration of *Alternaria* spores (ASIn) (Galán et al., 2017) in Bavaria. Start-and-end dates of the spore season for each location, if data were available for that site, were calculated with two different methods, the 95 % method (Goldberg et al., 1988) (Fig. 5-B) and the clinical method (Fig. 5-C), considering the threshold as of 100 spores/m³ in three consecutive days (Pfaar et al., 2017; Twaroch et al., 2015).

4. Discussion

In this study we present a U-net trained from scratch for the detection of *Alternaria* spores in BAA500 images. The BAA500, a fully automatic pollen monitor, overcomes the limitation of manual Hirst traps and comes close to real-time monitoring, providing data with a delay of 1 to 3 h instead of up to 7 days. This is desirable as the prevalence of pollinosis, a significant health problem, has increased steadily over the last decades and thus interest in current and real-time airborne concentrations has increased.

Up-to-date data allow medical doctors to make a more accurate diagnosis for patients that arrive for consultation with allergy symptoms and assist them to better cope with their disease. In addition, spore monitoring also benefits other fields, such as agriculture, where prompt knowledge of spore levels can help farmers to control pests in crops and thus avoid high economic losses (Iglesias et al., 2007), or climate change monitoring, which uses airborne spore levels as bioindicators (Hanson et al., 2022; Rojo et al., 2021), among others.

Since fungi depend on climatic conditions rather than photoperiod for their life cycle, the airborne behavior of their spores is even more likely to vary with climate change than other aerobiological particles (Cecchi et al., 2010; Gehrig and Clot, 2021). Shifts in the spore season related to climate change will impact allergic patients. For instance, the presence of spores and pollen matches the increase of allergic asthma episodes (Canova et al., 2013). Therefore, the completion and continuation of time series will allow a better study of spore trends and enable the establishment of health policies as elaborating forecasts (Grinn-Gofroñ et al., 2019; Tomassetti et al., 2009).

Although some studies show a slight decrease in fungal spore production (Damialis et al., 2015a, 2015b), there has been an increase in *Alternaria*

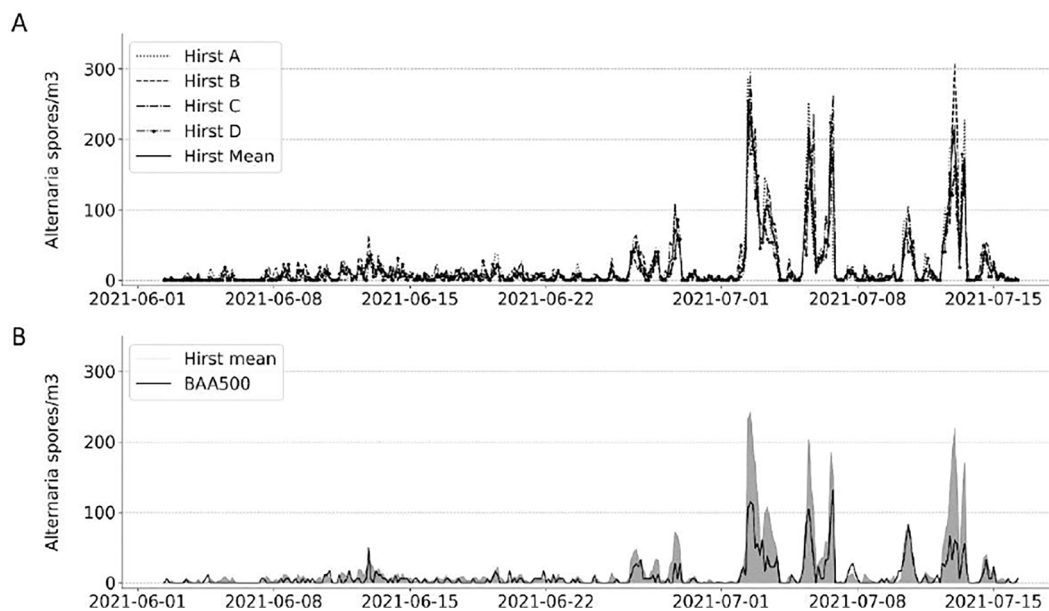


Fig. 4. Time series of *Alternaria* spore concentrations during the EUMETNET AutoPollen-COST ADOPT intercomparison campaign 2021, Munich (Germany), over the period 1.06.2021–14.07.2021. A) Time lines (3 h resolution) of *Alternaria* spore concentrations measured by each of the four Hirst traps (A,B,C,D) and the mean of the four Hirst traps. B) Time series (3 h resolution) of *Alternaria* spore concentrations of the mean of the four Hirst traps (grey shadow) versus the BAA500 values (black line) with a concentration factor of 5.5, (counted events to concentration) of the BAA500 values measured with the U-net.

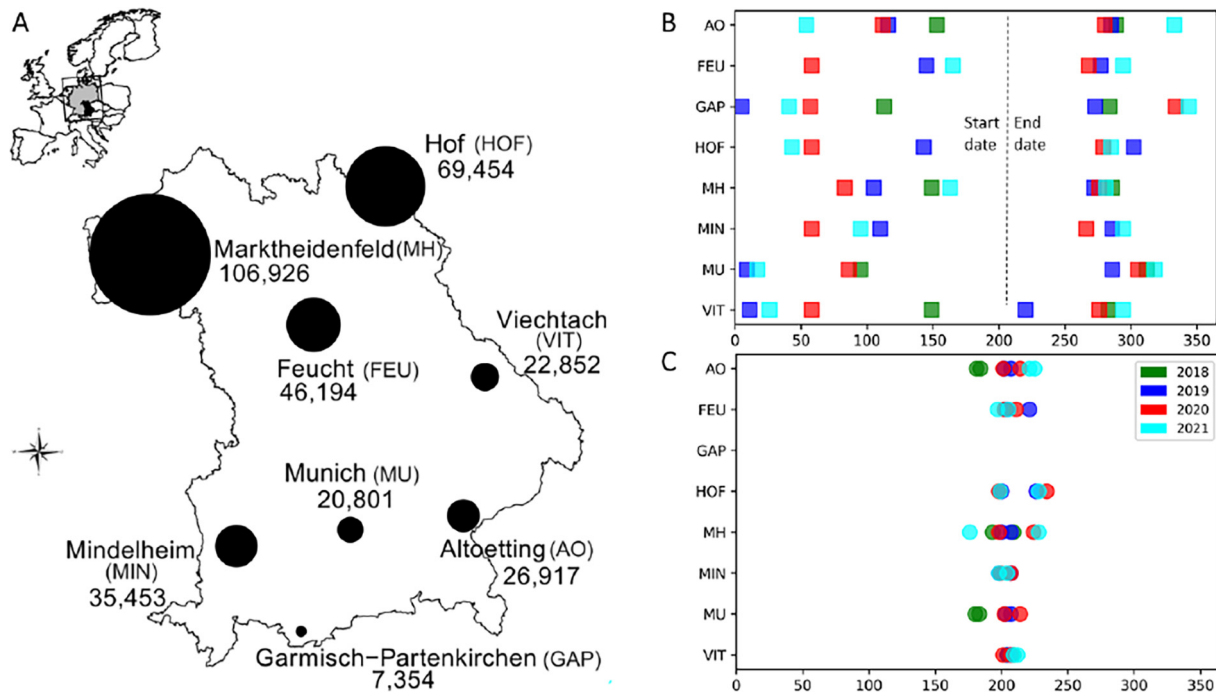


Fig. 5. Results of the re-analysis of the ePIN database. A) Map of Bavaria (Germany, Europe) representing the Annual Spore Integral (ASIn) for the eight stations of the ePIN network for the year 2021. B) Start and end dates represented as day of the year of the *Alternaria* spore season for each location and year sampled, calculated by the 95 % method (Goldberg et al., 1988) or C) the same but calculated according to a clinical definition for allergy symptoms (Pfaar et al., 2017). The vertical line is for orientation between start and end date.

sensitization, thus public alerts can prevent *Alternaria* allergy sufferers from being exposed to the airborne fungal allergens. Having long time series is important to being able to identify these trends, more importantly in cities, where pollution levels tend to be higher; pollutants such as diesel exhaust particles have been described to be allergen carriers as well (Knox et al., 1997). *Alternaria* shows peaks of airborne spores during summer, when pollutants that can exacerbate symptoms are present in higher concentrations due to favorable weather conditions, i.e. elevated ozone levels resulting from photochemical smog processes that irritate the respiratory tract. However, studies showing significant allergen-pollutant relations are still inconclusive (Bartra et al., 2007; Grewling et al., 2019; Lam et al., 2021).

The BAA500's image-based technology enables the storage of raw data and re-use of these data to develop new identification algorithms, widening its capabilities. Nonetheless, during the training step of the *Alternaria* classifier we encountered some technical problems, such as the lack of a large enough training data set or the occlusion of *Alternaria* spores (when particles are attached or behind other particles and segmentation algorithms have difficulties to find the particles of interest, i.e. *Alternaria* hiding in "junk").

The common problem of obtaining representative and large enough samples to train an algorithm for specific real-world applications (Khanzhina et al., 2022) was worsened by the fact that the *Alternaria* genus presents both a wide variety in morphology depending on the species, and within-species morphological changes along the maturation stages, resulting in the compilation of fewer examples per species in each maturation stage. We solved the problem by sampling randomly direct from nature (i.e. images from BAA500 from environmental samples all over Bavaria during the whole season) and by applying data augmentation techniques, as explained in the Materials and Methods section (Fig. 2) to avoid overfitting. This is a common technique when small datasets are used to train deep networks (Minaee et al., 2020). Data augmentation improved the detection algorithm from IoU = 0.93 to IoU = 0.95 when compared to the use of just raw images.

Some potential sources of bias and errors were also controlled. To increase efficiency when creating the *Alternaria* dataset, most of the examples

were taken during the summer months (July and August) when *Alternaria* levels are higher. While this could conceivably have biased the dataset, results in Test 2 (Table 1) showed that the algorithm performed well also in other months of the year across the eight different locations from the ePIN network.

Most of the surface of images photographed by the device are background pixels (97 %). This fact could have added another bias when assigning a class to each pixel in the image (background, *Alternaria* or other particle), but the problem was solved by giving higher weights to the *Alternaria* pixel-class (Minaee et al., 2020). Although there is room for improvement, results are promising. 'Internal tests' have achieved a precision, recall and F1 score of 0.92, 0.84 and 0.88, respectively.

Neural networks can extract features that may not be apparent to human vision. Conversely, some features that are clearly identifiable by humans may be difficult to detect by computers. Hence, we decided to scrutinize individual FP and FN cases in a random subsample of images to try to gain a better understanding of the network's hurdles. We encountered the common problem of occlusion (Ren et al., 2016). Although many spores attached to other particles were correctly detected (Fig. 3), some FN errors occurred when *Alternaria* spores were 'occluded' or attached to other particles, usually to inorganic particles or dust (*Alternaria* spores hidden in "junk"). Also, particles that look similar to *Alternaria* spores were confused by the algorithm. For example, half of the FP (4.2 %) were other spores such as *Bipolaris*, *Stemphylium*, *Pleospora* or *Triposporium*. All of them present longitudinal or transverse *septa* or have a similar shape (Fig. 6-A). Errors occurred also with elongated particles, usually fragments of vegetal tissues or hairs (Fig. 6-B).

Another repeated misclassification was found with the air vesicles of *Pinus* grains (Fig. 6-C), which usually appears around May when pine grains have a peak. While human vision can easily tell them apart, the algorithm could not. It may be that the grey colour-scheme or pixel organization confused the algorithm. However, despite clear cases of confusion, the misclassification was limited and accounted in our datasets to 8.4 % for FP.

As previously mentioned, the Hirst-type trap is considered the only current reference in pollen and spore monitoring, although it has some

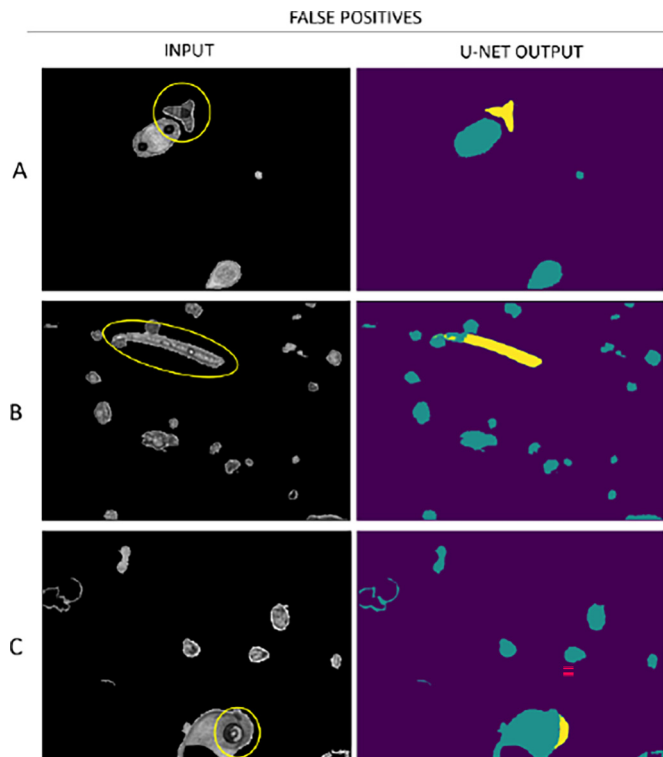


Fig. 6. Some examples of false positive U-net classifications (8.4 % of all classifications). A-C Left: input images of the BAA500. A-C Right: output of the U-net, falsely identified *Alternaria* spores (yellow patches). A) another spore, *Triposporium*, B) particle of vegetal origin, C) air vesicle of a *Pinus* pollen grain.

limitations. For instance, if the BAA500 reports different counts for a particle than a Hirst-type trap, we cannot be certain which instrument reports the correct values because to date it is not possible to calibrate instruments using any type of biological particle, including pollen and spores. The AIC aimed at evaluating the capabilities for the new automatic air monitoring devices and whether they diverge from Hirst traps' counts.

Although results from this campaign show peak counts of BAA500 and Hirst-type traps that correlated well ($R^2 = 0.78$), total counts were different. While a non-homogeneous distribution of pollen and spores over the sampling site could have potentially caused this divergence, a difference in capturing efficacy between Hirst and BAA500 is a more likely explanation, as the variability between the same Hirst traps is about 25 % but the difference between Hirst and BAA500 is larger. It is possible that the BAA500 does not capture all *Alternaria* spores present in ambient air, but this is difficult to assess. Perhaps the large size of *Alternaria* spores and their elongated shape might impact the sampling efficacy, as BAA500 has a more convoluted impactor than the Hirst traps. Or maybe the algorithm encountered more difficulties on recognizing *Alternaria* spores in early maturation stages than technicians, resulting in detecting lower concentrations.

Nevertheless, the correlation between Hirst-type and BAA500 is good, and the results of the analysis of the ePIN database show similar behavior to the historical presence of *Alternaria* spores, taking as an example the data from the city of Munich and thus, enabling the calculation of a scaling factor (factor to match Hirst-type counts) (Maya-Manzano et al., 2022; Smith et al., 2022). Although normally for pollen no scaling factor is used for BAA500 data, contrary to other automatic pollen monitors (Crouzy et al., 2016; Maya-Manzano et al., 2022), here due to probably the large size (sometimes $>50 \mu\text{m}$) and elongated shape of *Alternaria* spores as compared to the rounded shape of pollen grains, a scaling factor is needed. It is important to note that a scaling factor was different from a concentration factor. The concentration factor is used to convert the counted events (number of *Alternaria* spores) to concentration using the flowrate and photographed surface of the BAA500.

Some studies use a scaling factor to match the automatic counts to manual counts. This factor can be calculated as the 95th percentile of manual counts divided by the 95th percentile of the automatic counts (Maya-Manzano et al., 2022), which in our case is 1.92 for *Alternaria*. When this scaling factor was applied to the BAA500 data from the AIC, the total counts fitted well with the Hirst results (Fig. A.2). However, since Hirst-type traps themselves have limitations (Tummon et al., 2021b), adjusting counts alone might not solve the problem of obtaining real airborne spore concentrations. Nevertheless, it still enables us to draw continuous historical timelines. Thus, we have used the new algorithm to obtain *Alternaria* relative airborne levels since the installation of the automatic devices (2018) as if they would have been reported by Hirst-type traps (i.e. used the scaling factor).

In Fig. 5-A, the annual spore index (ASIn) over Bavaria is shown for the year 2021. This year was chosen since 2021 had data for the complete year from all stations. Although there are still not enough years of data to carry out a robust statistical analysis and to account for inter-annual variability, differences in the ASIn can be observed. Lower levels are seen towards the south, as expected, due to colder weather because of the proximity to the Alps and higher values in the warmer north of Bavaria.

5. Limitations and conclusion

We present a new algorithm able to detect airborne *Alternaria* spores, thus widening the functionality of the ePIN network. This is one of the first times a historical database from an automatic device is re-analyzed to get outputs of a fungal spore at the genus level (*Alternaria*). Our approach may have some limitations: the algorithm has difficulties when multiple *Alternaria* spores are stuck together (the occlusion problem), which is technically a challenging task to split into individual particles; but we were able to compute the number of False negatives for the validation set. It is feasible to validate a large dataset manually, by checking a small subset of images, in order to find undetected spores (false negatives), or false positives.

In spite of these limitations, *Alternaria* spores were correctly detected. The algorithm was applied to the complete time series (2018–2022), which might improve the diagnosis of allergies to *Alternaria*, an important health problem. The *Alternaria* time series can also be used in other fields such as climate change monitoring or pest control, in agriculture. Despite a high recognition rate of 0.92, the accuracy of this algorithm can nevertheless still be improved. Furthermore, this methodology could be adapted for other interesting taxa since it makes the BAA500 software more flexible and capable of adjusting to different bio-geographical areas with different species of interest.

Supplementary data to this article can be found online at <https://doi.org/10.1016/j.scitotenv.2022.160180>.

CRedit authorship contribution statement

Mónica Gonzalez-Alonso: conceptualization, data curation, writing-original draft preparation; Mihai Boldeanu: code, writing; Tom Koritnik: data curation; Jose Gonçalves: data curation; Lenz Belzner: code supervision; Tom Stemmler: code supervision; Robert Gebauer: code supervision and implementation; Lukasz Grewling: spore's counting; Fiona Tummon: campaign organization; Jose M. Maya-Manzano: data curation, campaign organization, supervision, writing; Arturo H. Ariño: Supervision, conceptualization, writing; Carsten Schmidt-Weber: supervision; Jeroen Buters: Supervision, conceptualization, coordination, funding and writing. All authors have reviewed the paper and agreed with the content.

Data availability

Data will be made available on request.

Declaration of competing interest

The authors report no conflict of interest. Tom Stemmler is currently working at Helmut Hund GmbH., however this had no effect on the results

presented as the investigations were carried out in compliance with good scientific practices.

Acknowledgements

We would like to thank the EUMETNET AutoPollen-COST ADOPT inter-comparison campaign, funded by the EUMETNET AutoPollen Programme and also including funding of the Bayerisches Landesamt für Gesundheit und Lebensmittelsicherheit (LGL) and from the COST Action CA18226 ADOPT (*New approaches in detection of pathogens and aeroallergens*). We thank the team who assisted in the EUMETNET AutoPollen-COST ADOPT intercomparison campaign 2021, specially the team lead by Łukasz Grewling in Poznan, Poland, and to Agata Szymanska and Łukasz Kostecki for counting the *Alternaria* spores from the Hirst traps. We also thank the Bayerisches Landesamt für Gesundheit und Lebensmittelsicherheit (LGL, Prof. Dr. Caroline Herr, Prof. Dr. Stephanie Heinze, Alica Weber, Susanna Kutzora, Katharina Heigl) for providing the data of the ePIN-Network. We would like to thank Stephan Hachinger for its help during the settings of the LRZ supercomputer analysis. Finally, also thanks to the group of people who helped in the annotation task of images (Alperen Özkan, Anastasia Tsoukala, Arno Claude, Borja Abascal, Jiakuan Zhao, Katalin Buday, Marina Muñoz Triviño, Marius Meinhold, Mateus Messias Mendes, Michal Mastalerz, Müge Molbay, Mykyta Yemelianovsky, Paul Pressler, Monica Gomez).

References

- Abascal, A., Rodríguez-Carreño, I., Vanhuyse, S., Georganos, S., Sliuzas, R., Wolff, E., Kuffer, M., 2022. Identifying degrees of deprivation from space using deep learning and morphological spatial analysis of deprived urban areas. *Comput. Environ. Urban. Syst.* 95. <https://doi.org/10.1016/j.compenvurbsys.2022.101820>.
- Alex, Krizhevsky, Sutskever Ilya, H.G.E., 2012. ImageNet classification with deep convolutional neural networks. *NIPS Papers*. <https://doi.org/10.2165/00129785-200404040-00005>.
- Bartra, J., Mollot, J., del Cuvillo, A., Dávila, I., Ferrer, M., Jáuregui, I., Montoro, J., Sastre, J., Valero, A., 2007. Air pollution and allergens. *J. Investig. Allergol. Clin. Immunol.* 17 (Suppl. 2), 3–8.
- Bishop, C.M., 1996. *Neural Networks: A Pattern Recognition Perspective*. <http://www.ncrc.aston.ac.uk/>.
- Boldeanu, M., Gonzalez-Alonso, M., Cucu, H., Burileanu, C., Maya-Manzano, J.M., Buters, J., 2022. Automatic pollen classification and segmentation using U-nets and synthetic data. *IEEE Access* 1–1. <https://doi.org/10.1109/ACCESS.2022.3189012>.
- Bozek, A., Pyrkosz, K., 2017. Immunotherapy of mold allergy: a review. *Hum. Vaccin. Immunother.* 13 (10), 2397–2401. <https://doi.org/10.1080/21645515.2017.1314404>.
- Buters, J.T.M., Antunes, C., Galveias, A., Bergmann, K.C., Thibaudon, M., Galán, C., Schmidt-Weber, C., Oteros, J., 2018. Pollen and spore monitoring in the world. *Clinical and translational. Allergy* 8 (1). <https://doi.org/10.1186/s13601-018-0197-8>.
- Canova, C., Heinrich, J., Anto, J.M., Leynaert, B., Smith, M., Kuenzli, N., Zock, J.P., Janson, C., Cerveri, I., de Marco, R., Toren, K., Gislason, T., Nowak, D., Pin, I., Wjst, M., Manfreda, J., Svanes, C., Crane, J., Abramson, M., Jarvis, D., 2013. The influence of sensitisation to pollens and moulds on seasonal variations in asthma attacks. *Eur. Respir. J.* 42 (4), 935–945. <https://doi.org/10.1183/09031936.00097412>.
- Cecchi, L., D'Amato, G., Ayres, J.G., Galan, C., Forastiere, F., Forsberg, B., Gerritsen, J., Nunes, C., Behrendt, H., Akdis, C., Dahl, R., Annesi-Maesano, I., 2010. Projections of the effects of climate change on allergic asthma: the contribution of aerobiology. *Allergy* 65 (9), 1073–1081. <https://doi.org/10.1111/j.1398-9995.2010.02423.x>.
- Chappuis, C., Tummon, F., Clot, B., Konzelmann, T., Calpini, B., Crouzy, B., 2020. Automatic pollen monitoring: first insights from hourly data. *Aerobiologia* 36, 159–170. <https://doi.org/10.1007/s10453-019-09619-6>.
- Clot, B., Gilge, S., Hajkova, L., Magyar, D., Scheifinger, H., Sofiev, M., Büttler, F., Tummon, F., 2020. The EUMETNET AutoPollen programme: establishing a prototype automatic pollen monitoring network in Europe. *Aerobiologia*. <https://doi.org/10.1007/s10453-020-09666-4> Special Issue Autopollen.
- Cramer, R., Garbani, M., Rhyner, C., Huitema, C., 2014. Fungi: the neglected allergenic sources. *Allergy* 69 (2), 176–185. <https://doi.org/10.1111/all.12325>.
- Crouzy, B., Stella, M., Konzelmann, T., Calpini, B., Clot, B., 2016. All-optical automatic pollen identification: towards an operational system. *Atmos. Environ.* 140, 202–212. <https://doi.org/10.1016/j.atmosenv.2016.05.062>.
- D'Amato, G., Cecchi, L., Bonini, S., Nunes, C., Annesi-Maesano, I., Behrendt, H., Liccardi, G., Popov, T., van Cauwenberge, P., 2007. Allergenic pollen and pollen allergy in Europe. *Allergy* 62 (9), 976–990. <https://doi.org/10.1111/j.1398-9995.2007.01393.x>.
- D'Amato, G., Chatzigeorgiou, G., Corsico, R., Gioulekas, D., Jäger, L., Jäger, S., Kontou-Fili, K., Kouridakis, S., Liccardi, G., Meriggi, A., Palma-Carlos, A., Palma-Carlos, M.L., Pagan Alemani, A., Parmiani, S., Puccinelli, P., Russo, M., Spiekma, F.T., Torricelli, R., Wüthrich, B., 1997. Evaluation of the prevalence of skin prick test positivity to *Alternaria* and *Cladosporium* in patients with suspected respiratory allergy A European multicenter study promoted by the Subcommittee on Aerobiology and Environmental Aspects of Inhalant Allergens of the European Academy of Allergology and Clinical Immunology. *Allergy* 52 (7), 711–716. <https://doi.org/10.1111/j.1398-9995.1997.tb01227.x>.
- Damialis, A., Mohammad, A.B., Halley, J.M., Gange, A.C., 2015. Fungi in a changing world: growth rates will be elevated, but spore production may decrease in future climates. *Int. J. Biometeorol.* 59 (9), 1157–1167. <https://doi.org/10.1007/s00484-014-0927-0>.
- Damialis, A., Vokou, D., Gioulekas, D., Halley, J.M., 2015. Long-term trends in airborne fungal-spore concentrations: a comparison with pollen. *Fungal Ecol.* 13, 150–156. <https://doi.org/10.1016/j.funeco.2014.09.010>.
- Delfino, R.J., Coate, B.D., Zeiger, R.S., Seltzer, J.M., Street, D.H., Koutrakis, P., 1996. Daily asthma severity in relation to personal ozone exposure and outdoor fungal spores. *Am. J. Respir. Crit. Care Med.* 154 (3), 633–641. <https://doi.org/10.1164/JRCCM.154.3.8810598>.
- Dutta, A., Gupta, A., Zisserman, A., 2019. VGG Image Annotator (VIA) 2.0.10. Open Software. <https://www.robots.ox.ac.uk/~vgg/software/via/>.
- Erb, S., Berne, A., Burgdorfer, N., Clot, B., Graber, M.-J., Lieberherr, G., Sallin, C., Tummon, F., Crouzy, B.B., 2022. Short communication: automatic real-time monitoring of fungal spores: the case of *Alternaria* spp. <https://doi.org/10.1101/2022.08.03.500168>.
- Forkel, S., Beutner, C., Schröder, S.S., Bader, O., Gupta, S., Fuchs, T., Schön, M.P., Geier, J., Buhl, T., 2021. Sensitization against fungi in patients with airway allergies over 20 years in Germany. *Int. Arch. Allergy Immunol.* 182 (6), 515–523. <https://doi.org/10.1159/000512230>.
- Galán, C., Smith, M., Thibaudon, M., Frenguelli, G., Oteros, J., Gehrig, R., Berger, U., Clot, B., Brandao, R., 2014. Pollen monitoring: minimum requirements and reproducibility of analysis. *Aerobiologia* 30 (4), 385–395. <https://doi.org/10.1007/s10453-014-9335-5>.
- Galán, C., Ariatti, A., Bonini, M., Clot, B., Crouzy, B., Dahl, A., Fernandez-González, D., Frenguelli, G., Gehrig, R., Isard, S., Levetin, E., Li, D.W., Mandrioli, P., Rogers, C.A., Thibaudon, M., Sauliene, I., Skjoth, C., Smith, M., Sofiev, M., 2017. Recommended terminology for aerobiological studies. *Aerobiologia* 33 (3), 293–295. <https://doi.org/10.1007/s10453-017-9496-0>.
- Gehrig, R., Clot, B., 2021. 50 years of pollen monitoring in Basel (Switzerland) demonstrate the influence of climate change on airborne pollen. *Front. Allergy* 2. <https://doi.org/10.3389/falgy.2021.677159>.
- Girshick, R., Donahue, J., Darrell, T., Malik, J., 2014. Rich Feature Hierarchies for Accurate Object Detection and Semantic Segmentation. <https://doi.org/10.48550/arXiv.1311.2524> ArXiv: 1311.2524v5.
- Goldberg, C., Buch, H., Moseholm, L., Weeke, E.R., 1988. Airborne pollen records in Denmark. 27 (3), 209–217. <https://doi.org/10.1080/00173138809428928>.
- Grewling, L., Nowak, M., Ska, A.S., Kostecki, L., Bogawski, P., 2019. Temporal variability in the allergenicity of airborne *alternaria* spores. *Med. Mycol.* 57 (4), 403–411. <https://doi.org/10.1093/mmy/myy069>.
- Grinn-Gofron, A., Strzelczak, A., Wolski, T., 2011. The relationships between air pollutants, meteorological parameters and concentration of airborne fungal spores. *Environ. Pollut.* 159 (2), 602–608. <https://doi.org/10.1016/J.ENVPOL.2010.10.002>.
- Grinn-Gofron, A., Nowosad, J., Bosiacka, B., Camacho, I., Pashley, C., Belmonte, J., de Linares, C., Janovici, N., Manzano, J.M.M., Sadyś, M., Skjoth, C., Rodinkova, V., Tormo-Molina, R., Vokou, D., Fernández-Rodríguez, S., Damialis, A., 2019. Airborne *alternaria* and *cladosporium* fungal spores in Europe: forecasting possibilities and relationships with meteorological parameters. *Sci. Total Environ.* 653, 938–946. <https://doi.org/10.1016/j.scitotenv.2018.10.419>.
- Hanson, M.C., Petch, G.M., Ottosen, T.B., Skjoth, C.A., 2022. Climate change impact on fungi in the atmospheric microbiome. *Sci. Total Environ.* 830. <https://doi.org/10.1016/j.scitotenv.2022.154491>.
- Hirst, J.M., 1952. An automatic volumetric spore trap. *Ann. Appl. Biol.* 39, 257–265.
- Iglesias, I., Rodríguez-Rajo, F.J., Méndez, J., 2007. Evaluation of the different *alternaria* prediction models on a potato crop in a limia (NW of Spain). *Aerobiologia* 23 (1), 27–34. <https://doi.org/10.1007/s10453-006-9045-8>.
- Kasprzyk, I., Rodinkova, V., Šaulienė, I., Ritenberga, O., Grinn-Gofron, A., Nowak, M., Sulborska, A., Kaczmarek, J., Weryszko-Chmielewska, E., Bilous, E., Jedryczka, M., 2015. Air pollution by allergenic spores of the genus *alternaria* in the air of central and eastern Europe. *Environ. Sci. Pollut. Res.* 22 (12), 9260–9274. <https://doi.org/10.1007/s11356-014-4070-6>.
- Kasprzyk, I., Ćwik, A., Kluska, K., Wójcik, T., Cariñanos, P., 2019. Allergenic pollen concentrations in the air of urban parks in relation to their vegetation. *Urban For. Urban Green.* 46. <https://doi.org/10.1016/j.ufug.2019.126486>.
- Khanzhina, N., Filchenkov, A., Minaeva, N., Novoselova, L., Petukhov, M., Kharisova, I., Pineava, J., Zamorin, G., Putin, E., Zamyatina, E., Shalyto, A., 2022. Combating data incompetence in pollen images detection and classification for pollinosis prevention. *Comput. Biol. Med.* 140. <https://doi.org/10.1016/j.combiomed.2021.105064>.
- Knox, R.B., Suphioglu, C., Taylor, P., Desatt, R., Watson, H.C., Pengt, J.L., Bursill, L.A., 1997. Major grass pollen allergen *lol p 1* binds to diesel exhaust particles: implications for asthma and air pollution. *Clin. Exp. Allergy* 27 (3), 246–251.
- Lam, H.C.Y., Jarvis, D., Fuentes, E., 2021. Interactive effects of allergens and air pollution on respiratory health: a systematic review. *Sci. Total Environ.* 757. <https://doi.org/10.1016/j.scitotenv.2020.143924>.
- Lizaso Baciaico, M.T., García, B.E., Gómez, B., Zabalegui, A., Rodríguez, M.J., Tabar, A.I., 2003. Tratamiento de la alergia a hongos. *An. Sist. Sanit. Navar.* 26 (Suppl. 2), 129–137. <https://doi.org/10.4321/s1137-66272003000400016>.
- Martínez-Canavate Burgos, A., Valenzuela-Soria, A., Rojo-Hernández, A., 2007. Immunotherapy with *Alternaria alternata*: present and future. *Allergol. Immunopathol.* 35 (6), 259–263. <https://doi.org/10.1157/13112993>.
- Maya-Manzano, J.M., Fernández-Rodríguez, S., Hernández-Trejo, F., Díaz-Pérez, G., Gonzalo-Garjón, Á., Silva-Palacios, I., Muñoz-Rodríguez, A.F., Tormo-Molina, R., 2012. Seasonal Mediterranean pattern for airborne spores of *alternaria*. *Aerobiologia* 28 (4), 515–525. <https://doi.org/10.1007/s10453-012-9253-3>.
- Maya-Manzano, J.M., et al., 2022. Comparing automatic pollen monitors with Hirst-type pollen traps for total and individual pollen classification. *Science of the Total Environment* In press. Submitted for publication.
- Minaee, S., Boykov, Y., Porikli, F., Plaza, A., Kehtarnavaz, N., Terzopoulos, D., 2020. Image Segmentation Using Deep Learning: A Survey. <http://arxiv.org/abs/2001.05566>.

- Oteros, J., Pusch, G., Weichenmeier, I., Heimann, U., Möller, R., Röseler, S., Traidl-Hoffmann, C., Schmidt-Weber, C., Buters, J.T.M., 2015. Automatic and online pollen monitoring. *Int. Arch. Allergy Immunol.* 167 (3), 158–166. <https://doi.org/10.1159/000436968>.
- Oteros, J., Buters, J., Laven, G., Röseler, S., Wachter, R., Schmidt-Weber, C., Hofmann, F., 2017. Errors in determining the flow rate of hirst-type pollen traps. *Aerobiologia* 33 (2), 201–210. <https://doi.org/10.1007/s10453-016-9467-x>.
- Oteros, J., Weber, A., Kutzora, S., Rojo, J., Heinze, S., Herr, C., Gebauer, R., Schmidt-Weber, C.B., Buters, J.T.M., 2020. An operational robotic pollen monitoring network based on automatic image recognition. *Environ. Res.* 191, 110031. <https://doi.org/10.1016/j.envres.2020.110031>.
- Pawankar, R., 2014. Allergic diseases and asthma: a global public health concern and a call to action. *World Allergy Organ. J.* 7, 12. <https://doi.org/10.1186/1939-4551-7-12>.
- Pfaar, O., Bastl, K., Berger, U., Buters, J., Calderon, M.A., Clot, B., Darsow, U., Demoly, P., Durham, S.R., Galán, C., Gehrig, R., Gerth van Wijk, R., Jacobsen, L., Klimek, L., Sofiev, M., Thibaudon, M., Bergmann, K.C., 2017. Defining pollen exposure times for clinical trials of allergen immunotherapy for pollen-induced rhinoconjunctivitis – an EAACI position paper. *Allergy* 72 (5), 713–722. <https://doi.org/10.1111/all.13092>.
- Picornell, A., Rojo, J., Trigo, M.M., Ruiz-Mata, R., Lara, B., Romero-Morte, J., Serrano-García, A., Pérez-Badía, R., Gutiérrez-Bustillo, M., Cervigón-Morales, P., Ferencova, Z., Morales-González, J., Sánchez-Reyes, E., Fuentes-Antón, S., Sánchez-Sánchez, J., Dávila, I., Oteros, J., Martínez-Bracero, M., Galán, C., Recio, M., 2022. Environmental drivers of the seasonal exposure to airborne alternaria spores in Spain. *Sci. Total Environ.* 823, 153596. <https://doi.org/10.1016/j.scitotenv.2022.153596>.
- Polling, M., Li, C., Cao, L., Verbeek, F., Belmonte, J., de Linares, C., Willemsse, J., Gravendeel, B., 2021. Automatic image classification using neural networks increases accuracy for allergenic pollen monitoring. *Sci. Rep.* <https://doi.org/10.21203/rs.3.rs-116766/v1>.
- Ren, S., He, K., Girshick, R., Sun, J., 2016. Faster R-CNN: Towards Real Time Object Detection With Region Proposal Networks. <https://doi.org/10.48550/arXiv.1506.01497>.
- Rojo, J., Oteros, J., Picornell, A., Maya-Manzano, J.M., Damialis, A., Zink, K., Werchan, M., Werchan, B., Smith, M., Menzel, A., Timpf, S., Traidl-Hoffmann, C., Bergmann, K.C., Schmidt-Weber, C.B., Buters, J., 2021. Effects of future climate change on birch abundance and their pollen load. *Glob. Chang. Biol.* 27 (22), 5934–5949. <https://doi.org/10.1111/gcb.15824>.
- Ronneberger, O., Fischer, P., Brox, T., 2015. U-Net: Convolutional Networks for Biomedical Image Segmentation. *Medical Image Computing and Computer-Assisted Intervention (MICCAI)*. 9351. Springer, LNCS, pp. 234–241. <http://lmb.informatik.uni-freiburg.de/>.
- Šaulienė, I., Šukienė, L., Daunys, G., Valiulis, G., Vaitkevičius, L., Matavulj, P., Brdar, S., Panic, M., Šikoparija, B., Clot, B., Crouzy, B., Sofiev, M., 2019. Automatic pollen recognition with the rapid-E particle counter: the first-level procedure, experience and next steps. *Atmos. Meas. Tech.* 12 (6), 3435–3452. <https://doi.org/10.5194/amt-12-3435-2019>.
- Šaulienė, I., Šukienė, L., Daunys, G., Valiulis, G., Vaitkevičius, L., 2021. Automatic particle detectors lead to a new generation in plant diversity investigation. *Not. Bot. Horti Agrobot. Cluj-Napoca* 49 (3), 1–12. <https://doi.org/10.15835/nbha49312444>.
- Sauvageat, E., Zeder, Y., Auderset, K., Calpini, B., Clot, B., Crouzy, B., Konzelmann, T., Lieberherr, G., Tummon, F., Vasilatou, K., 2019. Real-time pollen monitoring using digital holography. *Atmos. Meas. Tech.* <https://doi.org/10.5194/amt-2019-427>.
- Schmidhuber, J., 2015. Deep learning in neural networks: an overview. *Neural Netw.* 61, 85–117. <https://doi.org/10.1016/j.neunet.2014.09.003>.
- Sevillano, V., Holt, K., Aznarte, J.L., 2020. Precise automatic classification of 46 different pollen types with convolutional neural networks. *PLoS ONE* 15 (6). <https://doi.org/10.1371/journal.pone.0229751>.
- Shorten, C., Khoshgoftaar, T.M., 2019. A survey on image data augmentation for deep learning. *J. Big Data* 6 (1). <https://doi.org/10.1186/s40537-019-0197-0>.
- Simon-Nobbe, B., Denk, U., Pöll, V., Rid, R., Breitenbach, M., 2008. The spectrum of fungal allergy. *Int. Arch. Allergy Immunol.* 145 (1), 58–86. <https://doi.org/10.1159/000107578>.
- Simonyan, K., Zisserman, A., 2015. Very deep convolutional networks for large scale image recognition. *ICLR 2015 Conference Paper* <https://doi.org/10.2146/ajhp170251>.
- Smith, M., Matavulj, P., Mimić, G., Panić, M., Grewling, L., Šikoparija, B., 2022. Why should we care about high temporal resolution monitoring of bioaerosols in ambient air? *Sci. Total Environ.* 826. <https://doi.org/10.1016/j.scitotenv.2022.154231>.
- Spiekma, F., 2003. Airborne mould spores of allergenic importance. *Postepy Dermatol. Alergol.* 20 (4), 205–208.
- Szegedy, C., Toshev, A., Erhan, D., 2013. Deep Neural Networks for Object Detection. *NeurIPS Proceedings*.
- Tabar, A.I., Lizaso, M.T., García, B.E., Gómez, B., Echechipía, S., Aldunate, M.T., Madariaga, B., Martínez, A., 2008. Double-blind, placebo-controlled study of *Alternaria alternata* immunotherapy: clinical efficacy and safety. *Pediatr. Allergy Immunol.* 19 (1), 67–75. <https://doi.org/10.1111/j.1399-3038.2007.00589.x>.
- Tešendić, D., Boberić Krstičević, D., Matavulj, P., Brdar, S., Panić, M., Minić, V., Šikoparija, B., 2020. RealForAll: real-time system for automatic detection of airborne pollen. *Enterp. Inf. Syst.* 1–17. <https://doi.org/10.1080/17517575.2020.1793391>.
- Tomassetti, B., Angelosante Bruno, A., Pace, L., Verdecchia, M., Visconti, G., 2009. Prediction of alternaria and pleospora concentrations from the meteorological forecast and artificial neural network in L'Aquila, Abruzzo (Central Italy). *Aerobiologia* 25 (3), 127–136. <https://doi.org/10.1007/s10453-009-9117-7>.
- Triviño, M.M., Maya-Manzano, J.M., Tummon, F., Clot, B., Grewling, L., Schmidt-Weber, C., Buters, J., 2022. Resistance free flow adjustment of Hirst-type pollen traps reduces variability between traps. *Aerobiologia Submitted for publication*.
- Tummon, F., Adamov, S., Clot, B., Crouzy, B., Gysel-Beer, M., Kawashima, S., Lieberherr, G., Manzano, J., Markey, E., Moallemi, A., O'Connor, D., 2021a. A first evaluation of multiple automatic pollen monitors run in parallel. *Aerobiologia (Special Issue: Autopollen)* <https://doi.org/10.1007/s10453-021-09729-0>.
- Tummon, F., Arboledas, L.A., Bonini, M., Guinot, B., Hicke, M., Jacob, C., Kendrovski, V., McCairns, W., Petermann, E., Peuch, V., Pfaar, O., Sicard, M., Šikoparija, B., Clot, B., 2021b. The need for Pan-European automatic pollen and fungal spore monitoring: A stakeholder workshop position paper. *Clinical and Translational Allergy*, clt2.12015 <https://doi.org/10.1002/ctt2.12015>.
- Twaroch, T.E., Curin, M., Valenta, R., Swoboda, I., 2015. Mold allergens in respiratory allergy: from structure to therapy. *Allergy, Asthma and Immunology Research* 7 (3), 205–220. <https://doi.org/10.4168/aaair.2015.7.3.205> Korean Academy of Asthma, Allergy and Clinical Immunology.
- Vidal, C., Enrique, E., Gonzalo, A., Moreno, C., Tabar, A.I., Alcántara, M., Alonso, A., Antepará, I., Arias-Irigoyen, J., Armentia, A., Bartra, J., Beristain, A., Blanco, C., Cabañes, N., Campo, P., Cardona, V., Carretero, P., Castillo, R., Canaria, G., Vega, J.M., 2014. Diagnosis and allergen immunotherapy treatment of polysensitized patients with respiratory allergy in Spain: an allergists' consensus. *Clinical and Translational Allergy* 4 (1), 36. <https://doi.org/10.1186/2045-7022-4-36>.